Unifying the communicable disease spreading paradigm with Gompertzian growth

Matz Haugen[1,*] and Dorothea Gilbert[2]

[1]Abel X, Oslo, Norway
[2]Independent Researcher, Oslo, Norway
*matzhaugen@gmail.com

ABSTRACT

Recently, a number of studies have shown that cumulative mortality followed a Gompertz curve in the initial Coronavirus epidemic period, March-April 2020. We show that the Gompertz curve is incompatible with expected initial logistic growth curves as predicted by traditional Susceptible-Infected-Recovered (SIR) models, and propose a new theory which better explains the nature of the mortality characteristics based on an environmental stressor. Second, we show that for the Gompertz curve to emerge, the stressor has to act on everyone simultaneously, rejecting the possibility of a disease propagation stage. Third, we connect logistic growth with Gompertzian growth by augmenting the logistic growth equation with higher order interaction terms, and show that the SIR model is compatible with Gompertzian growth only when all nodes in the transmission network communicate with infinite speed and interaction. Crucially, this augmentation must be accompanied by causality-reversal where the source of growth is not the pool of infected but the pool of susceptible people. We thus find a novel bridge between logistic and Gompertzian growth, separate from the existing Richards model (also called θ-logistic growth).

Introduction

Traditional communicable disease spreading theory assumes a pathogen which infects the population through a network of transmission. Following this line of reasoning it can be theoretically shown that in the early stages of an epidemic, growth follows a logistic-like curve, where the very beginning exhibits exponential growth, and for which analytic and semi-analytic solutions have recently emerged[1–4]. A large body of research reveals how these models fit the recent mortality seen due to the Coronavirus epidemic[5–10].

However, instead of showing logistic-like growth, observed cumulative mortality in the initial period March-April 2020 exhibits almost perfect resemblance to Gompertzian growth[11,12] where the log-transformed cumulative mortality, or log-mortality for short, is exponentially *decreasing* in time,

$$\frac{d}{dt} \ln Y(t) = -\beta \ln \frac{Y(t)}{\tilde{Y}} + \nu, \tag{1}$$

with constants $\tilde{Y}$, β, and ν, and whose solution is given as

$$Y(t) = Y_\infty \left(\frac{Y_0}{Y_\infty} \right)^{e^{-\beta t}}, \tag{2}$$

where $Y_0 = Y(t=0)$ and $Y_\infty = Y(t \to \infty) = \tilde{Y} e^{\nu/\beta}$.

This phenomenon is recorded by others[13–17], showing Gompertz curves at national levels instead of the traditionally predicted logistic curves. These observations are made possible in part due to the increased cadence and quality of data acquisition compared with earlier epidemics. What is causing such a discrepancy between these observations and the current theory of communicable diseases[18]?

In addition to the characteristic patterns of these national mortality curves, other observations that conflict more generally with the communicable disease models are 1) the lack of correlation between population density and mortality (or infection) rates[19–23], 2) no clear association between inter-generational relationships and fatality rates[24], and 3) the widespread morbidity and mortality spikes seen during spring 2020 among birds[25], dogs[26], rabbits[27–29], elephants[30], and horses[31–34]. Many of these animal mortality spikes are not attributable to the coronavirus, but the question still remains why these spikes all occurred within the same timeframe. While these observations are not reconcilable within the current communicable disease paradigm, we present here an alternative theory that can reconcile all observations; a theory with fewer parameters than the most basic

communicable disease model. We will then present a novel bridge between these two paradigms which connects the logistic growth model with the Gompertzian growth model in an alternative to the parametrization given by Richard (1959)[35]; a bridge built on higher order interaction terms.

Simple communicable disease models

We start by reviewing this basic infectious disease model, namely the Susceptible-Infected-Recovered (SIR) model under a time-dependent infection/recovery rate ratio, $\phi(t)$[36], and show under what conditions the Gompertz curve could emerge. First assume a pool of susceptible people of size N evolving between the three states: susceptible, $S(t)$, recovered, $R(t)$ and infected, $I(t)$,

$$
\begin{aligned}
\frac{dS}{dt} &= -\beta \frac{IS}{N} \\
\frac{dI}{dt} &= \beta \frac{IS}{N} - \alpha I. \\
\frac{dR}{dt} &= \alpha I,
\end{aligned}
\tag{3}
$$

omitting the argument t in each variable for brevity and where α and β in this context signify recovery and infection rates.

A line of reasoning employed by Rypdal and Rypdal (2020)[14] to obtain the Gompertz curve is to linearize the SIR model by assuming both the number of infected, $I(t)$, and cumulative infected, $Y(t)$, are much less than the initial pool of susceptible people, $N \gg Y \geq I$, which seems well founded at the national level, viz.

$$
\frac{dY}{dt} = \beta I
\tag{4}
$$

$$
\frac{dI}{dt} = (\beta - \alpha)I = \alpha(\phi(t) - 1)I,
\tag{5}
$$

and where the number of recovered, $R(t)$, is under this linearization decoupled from the other variables.

They further assume the number of diseased is proportional to the number of cumulative infected, offset by a time lag, which allows us to use the same set of linearized equations to model the number of cumulative people diseased without loss of generality.

Due to this linearization, the infection/recovery ratio, $\phi(t)$, will have to change as a function of time to accommodate for the boundary conditions. And since I is a function of Y, we can combine Eq. 4 via an instantaneous relative growth rate, $\gamma(t) = dY(t)/(Y dt) = \beta I/Y$, in turn parameterized by a scaling factor, θ, representing the shape of the growth,

$$
\frac{dY}{dt} = \gamma(t)Y(t)
\tag{6a}
$$

$$
\gamma(t) = \frac{\gamma_\infty}{\theta}\left[1 - \left(\frac{Y}{Y_\infty}\right)^\theta\right],
\tag{6b}
$$

where $\gamma_\infty = \gamma(t \to \infty)$. This parametrization is the commonly used Richards growth curve[35], also called θ-logistic growth, and has been used by others[37]. Although not immediately justified in the communicable disease theory, one could imagine that θ represents non-linear network behavior[38]. Note that at $\theta = 1$, the traditional logistic growth curve is obtained, while at $\theta \to \infty$ we recover the exponential (Malthusian) explosion.

The observed Gompertzian mortality curves are realized in the limit $\theta \to 0$, with the relative growth rate,

$$
\gamma(t) = \lim_{\theta \to 0} \frac{\gamma_\infty}{\theta}\left[1 - \left(\frac{Y}{Y_\infty}\right)^\theta\right] = \gamma_\infty \ln \frac{Y_\infty}{Y}
\tag{7}
$$

At this limit the relative growth rate approaches infinity as $Y \to 0$, which seems odd under the hypothesis that the pathogen has just started spreading. The Gompertzian limit also implies a decreasing relative growth rate from the very first time point, which under the SIR model seems unlikely given the large pool of susceptible people in the beginning. One would rather expect a near-constant relative growth rate in the beginning due to a disease propagation stage. Rypdal and Rypdal (2020)[14] suggest that the decreasing relative growth rate is caused by social and political mitigating efforts, but these hardly justify such coherent and consistent mortality characteristics across countries, particularly with an exponentially decreasing growth rate. In fact, Wang et al. (2012)[39] showed that any values of $\theta < 1$ are not physically realistic under a similar SIR model as the one given above.

Perhaps a more likely scenario from which a Gompertz curve would emerge is the selective infection of central nodes in the transmission network resulting in an immediate decrease in relative growth. Herrmann and Schwartz (2020)[40] studied a networked SIR model on a variety of networks, but did not elaborate on a possible fit to a Gompertz curve. Estrada and Bartesaghi (2022)[41] found that the Gompertz can emerge in later stages of an SIS (Susceptible-Infected-Susceptible) model, but not in the beginning of an SIR-like model. Although it may be possible to realize Gompertzian growth from a special network, firm theoretical work has yet to be done to show this connection. We will touch upon how the Gompertz curve emerges from one such network below, under some caveats.

The extended SIR model family is almost Gompertzian

Without the linearization and the θ-parametrization of the Richards model, one can still almost obtain Gompertzian growth from the communicable disease models. Under a double-log transform of Eq. 2, the growth curve is a simple straight line which can be seen as a tell-tale sign of a Gompertz curve,

$$\ln\left(\ln\left(Y_\infty/Y\right)\right) = -\beta t + k, \tag{8}$$

with $k = \ln\ln\frac{Y_\infty}{Y_0}$. To show this, we follow Carletti et al. (2020)[5] and consider the extended version of the SIR the model by including a group of diseased, $D(t)$, such that $N = S(t) + I(t) + R(t) + D(t)$, also called the SIRD model. This requires an addition to our original set of equations 3, with an extra equation for the diseased group's growth at some rate δ relative to the current infected group,

$$\frac{dD}{dt} = \delta I. \tag{9}$$

Algebraic manipulations reveal that the diseased group is described by a single equation, viz.

$$\frac{dD}{dt} = \eta(1 - e^{-\xi D}) - \kappa D, \tag{10}$$

where $\eta = \delta N$, $\xi = \beta/(\delta N)$, $\kappa = \delta + \alpha$, and where N is again synonymous to the initial susceptible pool of people. This pool of people cannot be obtained from deaths alone, but can be inferred by assuming a known ratio between mortality and recovery rates, δ and α. However, when only modeling the diseased as we do here, knowledge of N is irrelevant and the three parameters in Eq. 10 are sufficient.

In the beginning of an epidemic one can assume small values of D and thus the SIRD model follows logistic growth with

$$\frac{dD}{dt} = cD(1 - D/K), \tag{11}$$

obtained with a second order expansion of the exponential term in Eq. 10 and with $c = \eta\xi - \kappa$ and $K = 2c/\eta\xi^2$. Both the SIR and SEIR model exhibits similar properties and their discrepancy with initial observations related to the Coronavirus epidemic has been noted by others[42].

Without this approximation, the full 3-parameters in Eq. 10 of the diseased group can show a curve quite close to a straight line in the double-log domain even in the initial observations, although there will always be a non-zero concavity (Fig. 1 and the SI Appendix). Meanwhile, even though the Gompertz model can be fit with a 3-parameter model as shown in Eq. 1, it can also be simplified to a 2-parameter model estimated through linear regression of log-mortality,

$$\frac{d}{dt}\ln Y(t) = -\beta\left[\ln Y(t) - \ln Y_\infty\right]. \tag{12}$$

Thus, through linear regression estimates, the Gompertz model mitigates the possibility of non-identifiability issues of the parameters[43].

The SIRD model above also considers average macroscopic behavior of an ensemble of microscopic units justified through mean-field theory[44] which does not consider network effects explicitly. Rather, all entities are connected and communicating instantaneously as shown by Mombach et al. (2002)[45]. However, even with such strong assumptions, it is odd that observed mortality never exhibits a stage of near-exponential growth as this macroscopic SIRD model predicts, but rather a constant negative slope in the double-log domain. We are thus prompted to look for another model which can explain the observed mortality patterns.

An alternative theory for observed mortality

An alternative line of reasoning that does not rely on the framework of communicable diseases is that the biosphere was perturbed by an external stressor, initiating a stress response to eventually bring mortality rates back to stability.

Inspired by De Lauro et al. (2014)[47], the stressor can be modeled as a multiplicative stochastic dampening term along with a countering force of the immune system. As with all multiplicative processes, it is convenient to log-transform mortality and work in a dimensionless space such that $F(t) = Y(t)/Y_\infty$ and $Z(t) = \ln F(t)$, from which a natural perturbation model emerges,

$$dZ(t) = -\beta Z(t)dt + \sqrt{\sigma}dW(t), \tag{13}$$

where $dW(t)$ is a delta-correlated Wiener process with zero mean, making $Z(t)$ a stochastic process. The first term on the right hand side represents the growth due to the stressor, while the second represents the stress response.

This perturbation model is called an Ornstein–Uhlenbeck process[48], where $Z(t)$ is Gaussian. It is also interpreted as Newton's equation of motion with friction and a random force (Langevin's equation), and a continuous version of an Auto-Regressive(1) model[49]. As argued by De Lauro et al. (2014)[47], the diffusion coefficient, σ, represents the strength of the perturbation. This is seen if we recast our perturbation model in terms of mortality while introducing a new parameter $C = \exp\left(-\frac{\sigma}{2\beta}\right)$, viz.

$$dF(t) = \left\{ \frac{\sigma}{2}F(t) - \beta F(t)\ln\left[\frac{F(t)}{C}\right] \right\} dt + \sqrt{\sigma}F(t)dW(t). \tag{14}$$

To obtain the deterministic observable, we first take the average in the log-domain (Eq. 13),

$$d\langle \ln F(t) \rangle = -\beta \langle \ln F(t) \rangle dt, \tag{15}$$

where the bra-ket notation signifies the averaging operation. Then we use the property that for the log-normal quantity $F(t)$, the average of its logarithm is the logarithm of the *median* quantity[50], where we denote the median of $F(t)$ as $M(t)$,

$$d\ln M(t) = -\beta \ln M(t)dt, \tag{16}$$

which corresponds with the familiar deterministic Gompertz differential equation in Eq. 1 with $Y(t) = Y_\infty M(t)$. Comparing the stochastic stressor σ in Eq. 14 with the deterministic growth equation in Eq. 1 gives $\nu = \sigma/2$, suggesting that the stressor is indeed the source of growth, while β is the growth-limiting factor. We also see that by comparing equations 6a and 7 with the stochastic counterpart in Eq. 14 that the final growth level is governed by the stressor magnitude,

$$\sigma = 2\gamma_\infty \ln Y_\infty. \tag{17}$$

Thus, a more parsimonious interpretation of the observations not reliant on a transmission network is that mortality was caused by a planetary perturbation, modeled as a random process, to which organisms gradually develop resistance at a geometric rate in the log-transformed domain[51,52], which is the natural transformation for many processes in nature[53]. Under this model, the distribution of the abundance of $F(t)$ is log-normal, a result that can be obtained by directly solving the stochastic equation 14[50,54], or from thermodynamic principles[55–57]. Intuitively, this is seen by noting that the solution to the perturbation model in the log-domain (Eq. 13) is Gaussian in the variable $Z(t)$, thus suggesting a log-normal distribution of $F(t)$. This implies that the central limit theorem applies to the log-domain.

Unifying the SIR model and the Gompertz model

The remarkable observation that the log-transformed domain is the natural one merits closer study. First, juxtapose the logistic model with the Gompertz model,

$$\dot{M} = \frac{d}{dt}M(t) = \beta M(t)(1 - M(t)) \quad \text{Logistic} \tag{18a}$$

$$\frac{d}{dt}\ln(M(t)) = -\beta \ln(M(t)) \qquad \text{Gompertz,} \tag{18b}$$

where $M(t)$ is deterministic.

In the logistic model, we recognize the rightmost side of the logistic equation as the transmission term in a SIR model, but also as a linear interaction term between the two macroscopic states. As mentioned earlier, this procedure is a mean field

approximation with an implied average interaction between the variables. Thus, all dynamics are governed by macroscopic deterministic variables parametrized by a transmission rate.

A microscopic solution could be modeled by splitting the system into N microscopic deterministic units, $M(t) \rightarrow x_1(t), x_2(t), ..., x_N(t)$, where the lower case x_i emphasizes the microscopic quality of the variables, and is here interpreted as probability of infection. From these microscopic units, macroscopic growth could be obtained by taking their arithmetic average,

$$M(t) = \frac{1}{N} \sum_i^N x_i(t). \tag{19}$$

Naturally, this simple arithmetic average treats each microscopic unit as an independent variable contributing to the macroscopic observable.

One could add network interaction necessitating a corresponding matrix version of Eq. 18a

$$\frac{dx_i}{dt} = \beta(1 - x_i) \sum_j a_{ij} x_j \quad \forall i, \tag{20}$$

using the shorthanded $x_i = x_i(t)$ and with a fixed correlation governed by the network's growth or infection rate, β, and adjacency matrix, $\{a_{i,j}\} = \mathbf{A} \in \mathbb{R}^{N \times N}$, a binary matrix with ones where the ith and j^{th} nodes are connected, and zeroes otherwise. Notice that there is an implied causality from the infected to the susceptible, which will become relevant below. Furthermore, a linear correlation between variables is seen as the partial derivatives of the instantaneous growth rate with respect to pairs of microscopic variables,

$$\frac{\partial^2 \dot{M}}{\partial x_i \partial x_j} = -\frac{\beta}{N} a_{i,j}. \tag{21}$$

Still, no Gompertz curve will emerge at the onset of the growth process. Estrada and Bartesaghi (2022)[41] provide further analysis on this topic.

In contrast, as discussed above, the Gompertz model is implied by a multiplicative stochastic process with a log-normal distribution in its abundance at any given point in time. A log-normal distribution of abundance implies that the log-domain is the natural domain in which the central limit theorem applies, thus implying correlated mortality growth through the geometric mean,

$$M(t) = \exp\left[\frac{1}{N} \sum_i \ln x_i(t)\right] = \left[\prod_i x_i(t)\right]^{\frac{1}{N}} \tag{22}$$

Under this model, correlation between entities is present at all orders in the original domain and all the nodes in the network communicate instantaneously.

Thus, the emergence of the Gompertz curve at the macroscopic level suggests that the system is correlated, or coherent, presumably as a result of the simultaneous exposure to the same underlying stressor, but also due to the implied log-normal nature of the microscopic entities, where multiplication replaces addition as the aggregating operator[53]. We can now further appreciate the Richards parametrization as a transition from non-collaborative to collaborative growth as $\theta \rightarrow 0$. This feature of θ was also obtained by Petroni et al. (2020)[38] by interpreting the $\theta-$logistic growth rate in Eq. 6 as non-linear resource availability dependent on the overall magnitude, $Y(t)$, with growth at $\theta \rightarrow 0$ named "maximally coherent". Molski and Konarski (2003)[58] made a similar observation that Gompertzian growth is the coherent state in a quantum mechanical system with a time-dependent potential, an interpretation which sheds further light on the temporal nature of the postulated stress response. This quantum mechanical system has also been used to describe coherent energy states of diatomic molecules in space[59]. In the field of quantum physics, *coherence* is a well-defined mathematical property first explored by Glauber (1963)[60] in the context of electromagnetic fields. The fact that we observe the Gompertz curve in both the microscopic quantum scales and the macroscopic national scales is noteworthy, and suggests that both systems share commonalities and means of communication.

Unification through a modified SIR model

It is also possible to reconcile the SIR model with the Gompertz curve. Inspired by the observation that in the linearized approximation there are only two coupled states, infected and susceptible, we augment the interaction term to higher orders.

Then, we reverse the causality where the population of infected are now dependent on the population of the susceptible instead of the other way around as in Eq. 20,

$$\frac{dx_i}{dt} = \beta x_i \sum_j a_{ij}(1 - x_j) \quad \forall i. \tag{23}$$

This crucial change is based on the environmental stressor hypothesis rather than a communicable disease assumption. Furthermore, we will for the sake of simplicity assume all nodes in the network have exactly one neighbor and that there exists a unique path between all nodes,

$$\sum_i a_{ij} = 1 \quad \forall j. \tag{24}$$

If we let $s_i = 1 - x_i$ be the probability of being susceptible, the augmented and causality-reversed SIR model infection term becomes

$$\frac{dx_i}{dt} = \beta x_i \sum_j a_{ij}(s_j + s_j^2/2 + ...) - \alpha x_i \quad \forall i, \tag{25}$$

Now use the Taylor series $s + s^2/2 + ... = -\ln(1 - s)$, viz.

$$\frac{dx_i}{dt} = -\beta x_i \sum_j a_{ij}\ln(1 - s_j) - \alpha = -\beta x_i \sum_j a_{ij}\ln x_j - \alpha x_i \quad \forall i, \tag{26}$$

As we are interested in the aggregate macroscopic behavior, we take averages in the log domain, exploit our setup where $\mathbf{A}$ is a single mapping from one node to another, and simplify to

$$\frac{d}{dt}\ln\left[\prod_i^N x_i\right]^{\frac{1}{N}} = -\beta \ln\left[\prod_i^N x_i\right]^{\frac{1}{N}} - \frac{\alpha}{N}\sum_i^N x_i. \tag{27}$$

If $\alpha \to 0$, then this equation will exhibit Gompertzian growth in the geometric ensemble average of microscopic units. An interpretation of α going to 0 could be that the limiting factor emerges purely from the growth rate without the need for a second growth-limiting parameter, in line with the previous crucial hypothesis of causality reversal stated above. One further simplification could be seen in equating the logarithm of the geometric mean with the logarithm of the median of the set of x_i to obtain Eq. 16,

$$\frac{d}{dt}\ln M(t) = -\beta \ln M(t). \tag{28}$$

Finally we are positioned to arrive at a closed form expression for a finite number of interaction terms in this modified logistic model, which represents the infection term in the SIR model. Working with a single unitless growth variable and omitting the multivariate network without loss of generality, we start with

$$\frac{d\ln x}{dt} = \sum_{i=1}^N s^i/i. \tag{29}$$

Using standard integrals we see that the multiple terms amount to a Gompertz growth term adjusted by a Hypergeometric function,

$$\begin{aligned} \sum_{i=1}^N s^i/i &= \int_s \sum_{i=0}^{N-1} s^i ds \\ &= \int_s \frac{1 - s^N}{1 - s} ds \\ &= -\frac{{}_1F_2(1, N+1, N+2; s)}{N+1} s^{N+1} - \ln(1 - s), \end{aligned}$$

where $_1F_2$ is Gauss' Hypergeometric function, and integration limits are indefinite. Putting this all together, the modified logistic function emerges as

$$\frac{d}{dt}\ln x(t) = -\frac{_1F_2(1,N+1,N+2;1-x(t))}{N+1}(1-x(t))^{N+1} - \ln x(t). \qquad (30)$$

Note that for $N = 1$, this becomes the standard logistic function, while higher order terms will move closer and closer to the Gompertz curve as the hypergerometric term goes to zero. This modification to the logistic function does not have a 1-to-1 correspondence with the Richards model, but serves instead as an alternative when encoding non-linear or collaborative growth effects (see Fig. 2).

Conclusion

In conclusion, we have shown that Gompertzian growth follows from infinite interactions between the susceptible and infected states, and that the perceived pathogen travels at infinite speed throughout the population, rejecting the possibility of a disease propagation stage through a perceived transmission network. In this vein, the Richards parameter, θ, is related although not identical to the number of higher-order interactions with the susceptible and the infected population in a SIR model[35], where infinite interactions corresponds to $\theta \to 0$.

We further show that the observed mortality across countries can be explained by a model where the biological system is stressed by a ubiquitous and simultaneous stressor eliciting a corresponding stress response through which gradual return to pre-epidemic conditions are mediated. The stressor is modeled as a stochastic perturbation in the log-transformed domain of effects where correlation between people or microscopic entities is present at all orders. From this model, we draw parallels between the coherent behavior of the population's mortality evolution during an epidemic and the spatial coherence of quantum mechanical systems, borrowing the definition of coherence from quantum physics[58].

Thus, we see growth on a spectrum: In one extreme we find non-collaborative growth models or models with parameterized linear interaction effects, and in the other extreme we see a field of microscopic entities coherently sharing information much like quantum entangled particles. The emergence of coherent quantum phenomena at the macroscopic level suggests that no longer can the microscopic world claim a monopoly on quantum physics, especially as it relates to biology[61]. One might be surprised to find that temporal evolution of human mortality during epidemics can behave like the spatial energy distribution of quantum coherent systems.

Methods

Estimating model parameters

The time-evolution of the SIRD and the Gompertz model are obtained with a Runge-Kutta algorithm, after first fitting parameters using non-linear least squares according to equations 1 and 10 in the text (see SI Appendix for details). Fitting is done using Python-Scipy's non-linear least squares algorithm with specified Jacobians and a 6-day windowed average of observed deaths, similar to the technique by Carletti et al.[5]. Observations are taken from the Github repository compiled by the Center for Systems Science and Engineering (CSSE) at Johns Hopkins University, Baltimore, USA[46].

The transmission rate is modeled as the product of $\eta\xi$ in Eq. 10, and its associated variance is obtained assuming a bi-normal relationship between the two parameters with cross-correlation ρ[62],

$$\text{Var}[\beta] = \text{Var}[\eta]\text{Var}[\xi](1+\rho^2) + \text{Var}[\xi]*\text{E}[\eta]^2 + \text{Var}[\eta]\text{E}[\xi]^2, \qquad (31)$$

where estimates are obtained by substituting the model parameters with those estimated through the technique outlined above.

Code Availability

Scripts used to produce the plots are downloadable in the form of a Jupyter notebook using Python from
https://nbviewer.org/urls/emf-research.fra1.digitaloceanspaces.com/gompertz/gompertz_vs_sird.ipynb

Competing interests

The authors declare no competing interests.

Author Contributions

M. A. Haugen: Conceptualization, Methodology, Software, Writing. D. Gilbert: Conceptualization, Reviewing and Editing.

References

1. Harko, T., Lobo, F. S. & Mak, M. Exact analytical solutions of the susceptible-infected-recovered (sir) epidemic model and of the sir model with equal death and birth rates. *Appl. Math. Comput.* **236**, 184–194 (2014).

2. Kröger, M. & Schlickeiser, R. Analytical solution of the SIR-model for the temporal evolution of epidemics. part a: time-independent reproduction factor. *J. Phys. A: Math. Theor.* **53**, 505601 (2020).

3. Schlickeiser, R. & Kröger, M. Analytical solution of the SIR-model for the temporal evolution of epidemics: part b. semi-time case. *J. Phys. A: Math. Theor.* **54**, 175601 (2021).

4. Heng, K. & Althaus, C. L. The approximately universal shapes of epidemic curves in the susceptible-exposed-infectious-recovered (SEIR) model. *Sci. Reports* **10**, 1–6 (2020).

5. Carletti, T., Fanelli, D. & Piazza, F. COVID-19: The unreasonable effectiveness of simple models. *Chaos, Solitons & Fractals: X* **5**, 100034 (2020).

6. Cooper, I., Mondal, A. & Antonopoulos, C. G. A SIR model assumption for the spread of COVID-19 in different communities. *Chaos, Solitons & Fractals* **139**, 110057 (2020).

7. Postnikov, E. B. Estimation of COVID-19 dynamics "on a back-of-envelope": Does the simplest SIR model provide quantitative parameters and predictions? *Chaos, Solitons & Fractals* **135**, 109841 (2020).

8. Muñoz-Fernández, G. A., Seoane, J. M. & Seoane-Sepúlveda, J. B. A SIR-type model describing the successive waves of COVID-19. *Chaos, Solitons & Fractals* **144**, 110682 (2021).

9. Cooper, I., Mondal, A., Antonopoulos, C. G. & Mishra, A. Dynamical analysis of the infection status in diverse communities due to COVID-19 using a modified SIR model. *Nonlinear Dyn.* 1–14 (2022).

10. Saikia, D., Bora, K. & Bora, M. P. COVID-19 outbreak in india: an SEIR model-based analysis. *Nonlinear Dyn.* **104**, 4727–4751 (2021).

11. Gompertz, B. XXIV. on the nature of the function expressive of the law of human mortality, and on a new mode of determining the value of life contingencies. in a letter to francis baily, esq. f. r. s. &c. *Philos. Transactions Royal Soc. Lond.* **115**, 513–583, DOI: 10.1098/rstl.1825.0026 (1825).

12. Bajzer, Ž., Vuk-Pavlović, S. & Huzak, M. Mathematical modeling of tumor growth kinetics. In *A survey of models for tumor-immune system dynamics*, 89–133 (Springer, 1997).

13. Ohnishi, A., Namekawa, Y. & Fukui, T. Universality in COVID-19 spread in view of the gompertz function. *Prog. Theor. Exp. Phys.* **2020**, DOI: 10.1093/ptep/ptaa148 (2020).

14. Rypdal, K. & Rypdal, M. A parsimonious description and cross-country analysis of COVID-19 epidemic curves. *Int. J. Environ. Res. Public Heal.* **17**, 6487, DOI: 10.3390/ijerph17186487 (2020).

15. Català, M. *et al.* Empirical model for short-time prediction of COVID-19 spreading. *PLOS Comput. Biol.* **16**, e1008431, DOI: 10.1371/journal.pcbi.1008431 (2020).

16. Rodrigues, T. & Helene, O. Monte carlo approach to model COVID-19 deaths and infections using gompertz functions. *Phys. Rev. Res.* **2**, 043381 (2020).

17. Levitt, M., Scaiewicz, A. & Zonta, F. Predicting the trajectory of any COVID19 epidemic from the best straight line. *medRxiv* DOI: 10.1101/2020.06.26.20140814 (2020).

18. Castro, M., Ares, S., Cuesta, J. A. & Manrubia, S. The turning point and end of an expanding epidemic cannot be precisely forecast. *Proc. Natl. Acad. Sci.* **117**, 26190–26196 (2020).

19. Hamidi, S., Sabouri, S. & Ewing, R. Does density aggravate the COVID-19 pandemic? *J. Am. Plan. Assoc.* **86**, 495–509, DOI: 10.1080/01944363.2020.1777891 (2020).

20. Hamidi, S., Ewing, R. & Sabouri, S. Longitudinal analyses of the relationship between development density and the COVID-19 morbidity and mortality rates: Early evidence from 1,165 metropolitan counties in the united states. *Heal. & Place* **64**, 102378, DOI: 10.1016/j.healthplace.2020.102378 (2020).

21. Carozzi, F. Urban density and covid-19. *SSRN Electron. J.* DOI: 10.2139/ssrn.3643204 (2020).

22. Khavarian-Garmsir, A. R., Sharifi, A. & Moradpour, N. Are high-density districts more vulnerable to the COVID-19 pandemic? *Sustain. Cities Soc.* **70**, 102911 (2021).

23. Barak, N., Sommer, U. & Mualam, N. Urban attributes and the spread of COVID-19: The effects of density, compliance and socio-political factors in israel. *Sci. Total. Environ.* **793**, 148626 (2021).

24. Arpino, B., Bordone, V. & Pasqualini, M. No clear association emerges between intergenerational relationships and COVID-19 fatality rates from macro-level analyses. *Proc. Natl. Acad. Sci.* **117**, 19116–19121, DOI: 10.1073/pnas.2008581117 (2020).

25. Fischer, L. *et al.* Increased mortality in wild tits in north rhine-westphalia (germany) in 2020 with a special focus on suttonella ornithocola and other infectious pathogens. *Eur. J. Wildl. Res.* **67**, DOI: 10.1007/s10344-021-01500-7 (2021).

26. Perisé-Barrios, A. J. *et al.* Humoral responses to SARS-CoV-2 by healthy and sick dogs during the COVID-19 pandemic in spain. *Vet. Res.* **52**, DOI: 10.1186/s13567-021-00897-y (2021).

27. Duff, P. *et al.* Disease surveillance in england and wales, december 2019. *Vet. Rec.* **186**, 15–16, DOI: 10.1136/vr.m68 (2020).

28. Hu, B. *et al.* Emergence of rabbit haemorrhagic disease virus 2 in china in 2020. *Vet. Medicine Sci.* **7**, 236–239, DOI: 10.1002/vms3.332 (2020).

29. Fukui, H., Shimoda, H., Kadekaru, S., Henmi, C. & Une, Y. Rabbit hemorrhagic disease virus type 2 epidemic in a rabbit colony in japan. *J. Vet. Med. Sci.* **83**, 841–845, DOI: 10.1292/jvms.21-0007 (2021).

30. van Aarde, R. J., Pimm, S. L., Guldemond, R., Huang, R. & Maré, C. The 2020 elephant die-off in botswana. *PeerJ* **9**, e10686, DOI: 10.7717/peerj.10686 (2021).

31. Kambayashi, Y. *et al.* Outbreak of equine coronavirus infection among riding horses in tokyo, japan. *Comp. Immunol. Microbiol. Infect. Dis.* **77**, 101668, DOI: 10.1016/j.cimid.2021.101668 (2021).

32. King, S. *et al.* Outbreak of african horse sickness in thailand, 2020. *Transboundary Emerg. Dis.* DOI: 10.1111/tbed.13701 (2020).

33. Lu, G. *et al.* African horse sickness: Its emergence in thailand and potential threat to other asian countries. *Transboundary Emerg. Dis.* DOI: 10.1111/tbed.13625 (2020).

34. Castillo-Olivares, J. African horse sickness in thailand: Challenges of controlling an outbreak by vaccination. *Equine Vet. J.* **53**, 9–14, DOI: 10.1111/evj.13353 (2020).

35. Richards, F. A flexible growth function for empirical use. *J. experimental Bot.* **10**, 290–301 (1959).

36. Kermack, W. O. & McKendrick, A. G. A contribution to the mathematical theory of epidemics. *Proc. royal society london. Ser. A, Containing papers a mathematical physical character* **115**, 700–721 (1927).

37. Wu, K., Darcet, D., Wang, Q. & Sornette, D. Generalized logistic growth modeling of the covid-19 outbreak: comparing the dynamics in the 29 provinces in china and in the rest of the world. *Nonlinear dynamics* **101**, 1561–1581 (2020).

38. Petroni, N. C., De Martino, S. & De Siena, S. Logistic and θ-logistic models in population dynamics: General analysis and exact results. *J. Phys. A: Math. Theor.* **53**, 445005 (2020).

39. Wang, X.-S., Wu, J. & Yang, Y. Richards model revisited: Validation by and application to infection dynamics. *J. theoretical biology* **313**, 12–19 (2012).

40. Herrmann, H. A. & Schwartz, J.-M. Why COVID-19 models should incorporate the network of social interactions. *Phys. Biol.* **17**, 065008 (2020).

41. Estrada, E. & Bartesaghi, P. From networked SIS model to the gompertz function. *Appl. Math. Comput.* **419**, 126882 (2022).

42. Vattay, G. Forecasting the outcome and estimating the epidemic model parameters from the fatality time series in COVID-19 outbreaks. *Phys. Biol.* **17**, 065002 (2020).

43. Roda, W. C., Varughese, M. B., Han, D. & Li, M. Y. Why is it difficult to accurately predict the COVID-19 epidemic? *Infect. disease modelling* **5**, 271–281 (2020).

44. Smilkov, D., Hidalgo, C. A. & Kocarev, L. Beyond network structure: How heterogeneous susceptibility modulates the spread of epidemics. *Sci. reports* **4**, 1–7 (2014).

45. Mombach, J. C., Lemke, N., Bodmann, B. E. & Idiart, M. A. P. A mean-field theory of cellular growth. *EPL (Europhysics Lett.* **59**, 923 (2002).

46. Dong, E., Du, H. & Gardner, L. An interactive web-based dashboard to track COVID-19 in real time. *The Lancet infectious diseases* **20**, 533–534 (2020).

47. De Lauro, E., De Martino, S., De Siena, S. & Giorno, V. Stochastic roots of growth phenomena. *Phys. A: Stat. Mech. its Appl.* **401**, 207–213 (2014).

48. Risken, H. *The Fokker-Planck Equation* (Springer, 1996).

49. Akaike, H. Statistical predictor identification. *Annals institute Stat. Math.* **22**, 203–217 (1970).

50. Petroni, N. C., De Martino, S. & De Siena, S. Gompertz and logistic stochastic dynamics: Advances in an ongoing quest. *arXiv preprint arXiv:2002.06409* (2020).

51. Boxenbaum, H. Hypotheses on mammalian aging, toxicity, and longevity hormesis: Explication by a generalized gompertz function. In *Biological Effects of Low Level Exposures to Chemicals and Radiation*, 1–39 (CRC Press, 2017).

52. Neafsey, P. J., Boxenbaum, H., Ciraulo, D. A. & Fournier, D. J. A gompertz age-specific mortality rate model of aging, hormesis, and toxicity: Fixed-dose studies. *Drug metabolism reviews* **19**, 369–401 (1988).

53. Zhang, C.-L. & Popp, F.-A. Log-normal distribution of physiological parameters and the coherence of biological systems. *Med. Hypotheses* **43**, 11–16 (1994).

54. Skiadas, C. H. Exact solutions of stochastic differential equations: Gompertz, generalized logistic and revised exponential. *Methodol. Comput. Appl. Probab.* **12**, 261–270 (2010).

55. Sitaram, B. & Varma, V. Statistical mechanics of the gompertz model of interacting species. *J. theoretical biology* **110**, 253–256 (1984).

56. Gunasekaran, N. & Pande, L. Log normal distribution for the intrinsic abundance of species from the gompertz model. *J. Theor. Biol.* **98**, 301–305 (1982).

57. Chakrabarti, C. & Bhadra, S. Non equilibrium thermodynamics and stochastics of gompertzian growth. *J. Biol. Syst.* **4**, 151–157, DOI: doi.org/10.1142/S0218339096000119 (1996).

58. Molski, M. & Konarski, J. Coherent states of gompertzian growth. *Phys. review E* **68**, 021916 (2003).

59. Morse, P. M. Diatomic molecules according to the wave mechanics. ii. vibrational levels. *Phys. review* **34**, 57 (1929).

60. Glauber, R. J. Coherent and incoherent states of the radiation field. *Phys. Rev.* **131**, 2766 (1963).

61. Lambert, N. *et al.* Quantum biology. *Nat. Phys.* **9**, 10–18 (2013).

62. Nadarajah, S. & Pogány, T. K. On the distribution of the product of correlated normal random variables. *Comptes Rendus Math.* **354**, 201–204 (2016).
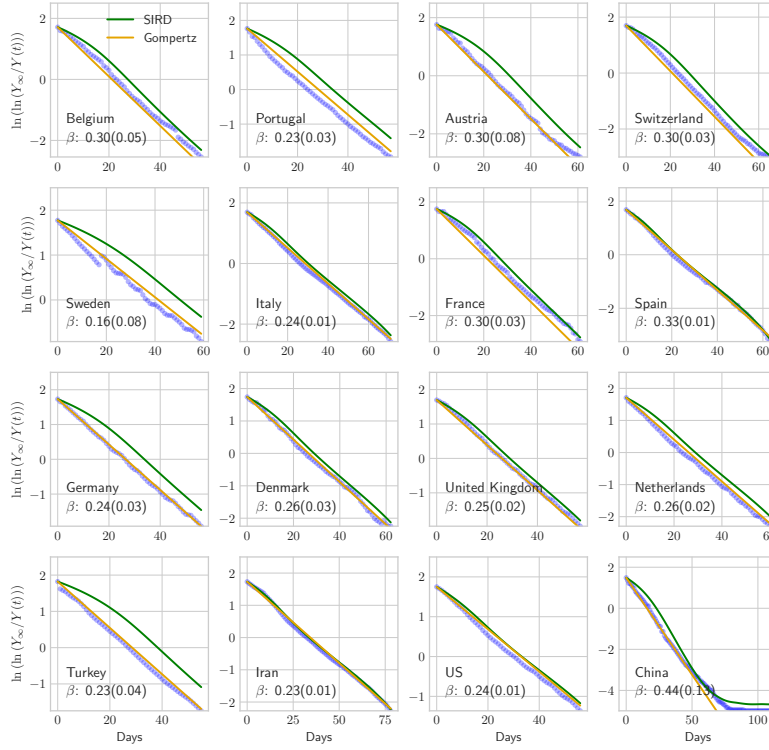
Figure 1. Cumulative number of diseased from the Coronavirus, transformed by $g(Y) = \ln\ln(Y_\infty/Y(t))$ plotted against number of days elapsed after $Y(t)/Y_{max} > 0.005$, comparing a SIRD model (green) with a Gompertz model (yellow) for a variety of countries in the period Jan-May 2020. Both models are fit using non-linear least squares according to equations 1 and 10 in the text. Although the Gompertz curve can also be obtained with a simple linear fit using Eq. 12, it is here obtained using non-linear least squares to put both models on equal footing. The temporal evolution of the SIRD model is obtained from the Runge-Kutta algorithm, while the Gompertz has a closed form for its temporal evolution. Each plot is annotated with an inferred transmission rate in the SIRD model with 1 standard deviation in brackets, assuming bi-normally distributed parameter estimates. Fitting is done with Python-Scipy and a 6-day moving average of deaths. Observations are taken from the Github repository compiled by the Center for Systems Science and Engineering (CSSE) at Johns Hopkins University, Baltimore, USA[46].
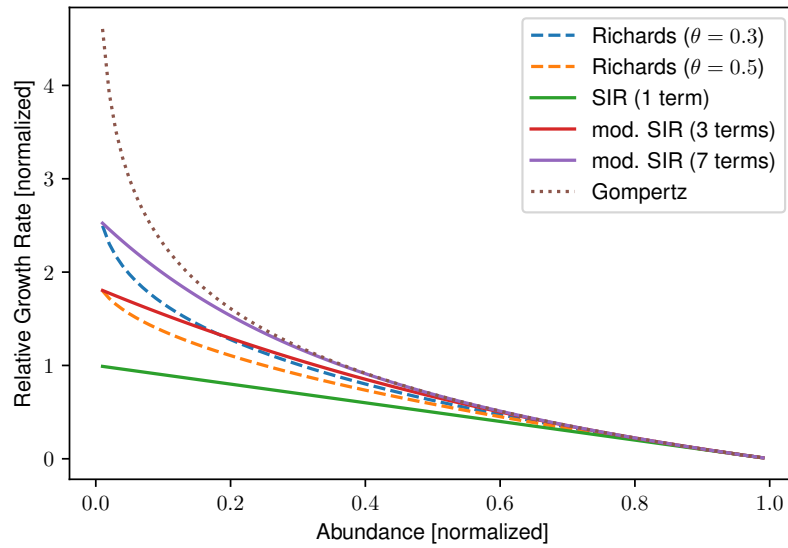
Figure 2. Comparison relative growth rate in the Richards θ-logistic model (Eq. 6), Gompertz model (Eq. 16), and the augmented causality-reversed SIR model (Eq. 30), all as a function of the abundance variable. Both dependent and independent variables are normalized so that final abundance (or size) is set to unity. The Richards θ-parameter is annotated in brackets in the legend, in addition to the number of terms used in the modified SIR model.